

Accurate estimation of feature importance faithfulness for tree models

Mateusz Gajewski^{*2,3}, Adam Karczmarz^{†1,2}, Mateusz Rapicki^{‡1}, and Piotr Sankowski^{§1,2}

¹Faculty of Mathematics, Informatics and Mechanics
University of Warsaw, Warsaw, Poland

²IDEAS NCBR

³Faculty of Computing and Telecommunications
Poznan University of Technology, Poznan, Poland

Abstract

In this paper, we consider a perturbation-based metric of predictive faithfulness of feature rankings (or attributions) that we call *PGI squared*. When applied to decision tree-based regression models, the metric can be computed accurately and efficiently for arbitrary independent feature perturbation distributions. In particular, the computation does not involve Monte Carlo sampling that has been typically used for computing similar metrics and which is inherently prone to inaccuracies.

Moreover, we propose a method of ranking features by their importance for the tree model’s predictions based on PGI squared. Our experiments indicate that in some respects, the method may identify the globally important features better than the state-of-the-art SHAP explainer.

1 Introduction

One of the key challenges in deploying modern machine learning models in such areas as medical diagnosis lies in the ability to indicate why a certain prediction has been made. Such an indication may be of critical importance when a human decides whether the prediction can be relied on. This is one of the reasons various aspects of explainability of machine learning models have been the subject of extensive research lately (see, e.g., [BH21]).

For some basic types of models (e.g., single decision trees), the rationale behind a prediction is easy to understand by a human. However, predictions of more complex models (that offer much better accuracy, e.g., based on neural networks or decision tree ensembles) are also much more difficult to interpret. Accurate and concise explanations understandable to humans might not always exist. In such cases, it is still beneficial to have methods *giving a flavor* of what factors might have influenced the prediction the most.

Local feature attribution¹ constitutes one of such general approaches. For a fixed input x and the model’s prediction $f(x)$, each feature is assigned a weight “measuring” the feature’s impact on the prediction. Ideally, a larger (absolute) weight should correspond to a larger importance of the feature for the prediction.

*mateusz.gajewski@ideas-ncbr.pl

†a.karczmarz@mimuw.edu.pl

‡mateusz.rapicki@mimuw.edu.pl

§piotr.sankowski@ideas-ncbr.pl

¹It should be contrasted with *global* feature attribution whose aim is to measure the feature’s total impact on the model.

Many local attribution methods have been proposed so far, e.g., [LL17, PMT18, RSG16]. They are often completely model-agnostic, that is, they can be defined for and used with any model which is only accessed in a black-box way for computing the attribution. In some of these cases, focusing on a particular model’s architecture can lead to much more efficient and accurate attribution computation algorithms (e.g., [LEC+20] for tree ensemble models).

With the large body of different attribution methods, it is not clear which one should one use, especially since there is not a single objective measure of their reliability. To help deal with this issue, several notions of explanation quality have been proposed in the literature, such as faithfulness (fidelity) [LKWN21, YHS+19], stability [AMJ18], or fairness [BZH+22, DUA+22]. [AKS+22] developed an open-source benchmark OpenXAI automatically computing variants of these measures for a number of proposed attribution methods.

Out of these notions, our focus in this paper is on faithfulness.

Roughly speaking, an attribution method deserves to be called faithful if the features deemed important by the attribution are truly important for the decision-making process of the model. The *perturbation-based* methods constitute one popular class of approaches to measuring faithfulness. Intuitively, perturbing features deemed impactful should generally lead to a significant change in the prediction. On the contrary, manipulating unimportant features should not make a big difference.

One concrete cleanly-defined perturbation-based faithfulness metric for regression problems is the *prediction gap on important feature perturbation*, PGI in short. PGI is a faithfulness measure of choice in the OpenXAI benchmark [AKS+22]. Having fixed some subset of important features S derived from the obtained attribution, the *prediction gap* wrt. S is defined as the expected absolute change in the prediction when an independent Gaussian noise is applied to each coordinate x_j , $j \in S$. PGI can be defined as either the prediction gap wrt. a fixed set of important features (e.g., k top-scoring features for some fixed k [DUA+22]), or an average prediction gap over many important feature sets (as in [AKS+22]). In particular, the PGI metric depends *only* on the ordering of features by importance induced by the attribution. Other perturbation-based methods include e.g., PGU [AKS+22], comprehensiveness, sufficiency [DJR+20], remove-and-retrain [HEKK19], deletion [PDS18].

In practice, PGI and other methods using random perturbations are computed using the Monte Carlo method which is inherently prone to inaccuracies, unless a very large number of samples is used.

It is interesting to ask whether PGI or similar random perturbation-based faithfulness matrices can be computed more accurately, say, with the approximation error caused merely by the floating-point arithmetic’s rounding errors.

1.1 Our contribution

1.1.1 Exact computation

First, we consider random perturbation-based measurement of faithfulness from the point of view of efficient and accurate computation. Of course, it is unrealistic to assume that such a quantity can be computed exactly (or even beyond the Monte Carlo method) given only black-box access to the model and the perturbation distribution. Hence, we focus on a concrete model architecture: tree ensemble models. Tree ensemble models remain a popular choice among practitioners since they are robust, easy to tune, and fast to train.

Unfortunately, computing the *prediction gap*, as defined in [AKS+22] (wrt. a fixed set S of perturbed features, see Section 2 for a formal definition), does not look very tractable given the rich structure that tree ensemble models offer. This is because therein, the expectation is taken over the *absolute value* of $f(x) - f(x')$, where x' is x with important features perturbed. The absolute value is not very mathematically convenient to work with when combined with expectations. On the other hand, dropping the absolute value here would not make much sense: a small random perturbation (positive or negative) of a feature could in principle lead to a large positive or negative prediction difference. These, in turn, could cancel out in expectation, making the metric close to zero even though the feature is visibly of high importance.

To deal with the tractability problem of measuring PGI on tree models, we propose a similar metric, PGI², where instead of taking the absolute value, we compute the expectation of the square prediction gap

$(f(x) - f(x'))^2$. This eliminates the cancellation problem outlined above. Of course, introducing the square can alter the evaluation of the feature’s importance wrt. PGI as defined previously. However, intuitively, it amplifies the big prediction differences, and at the same time marginalizes the small, which is a generally good property if we seek concise explanations.

We prove that for tree ensemble models with n nodes in total, the squared prediction gap can be computed in $O(n^2)$ time exactly for any fixed choice of subset of perturbed important features, assuming the cumulative distribution function of feature-wise random perturbations can be evaluated in constant time. That is, the obtained running time bound does not require that the random perturbations are Gaussian or their distributions are equal across features.

The OpenXAI benchmark calculates PGI by taking the average expected prediction gap obtained when perturbing $1, 2, \dots, d$ most important features (where d denotes the total number of features; see [AKS⁺22, Appendix A]). In such a case, d different expectations of absolute prediction gap are estimated, each of them via Monte Carlo sampling. In our case, PGI^2 is defined as the average expected squared prediction gap when perturbing $1, 2, \dots, d$ most important features. Using our prediction gap algorithm, PGI^2 is computed exactly (assuming infinite precision arithmetic; in reality, up to the precision error incurred by the usage of floating-point arithmetic) in $O(n^2d)$ time.

Experiments. We accompany our theoretical development with an experimental comparison of the results obtained using the exact algorithm and Monte Carlo sampling.

The experiments confirm that Monte Carlo simulation gives noticeably less accurate results within the allocated time (iteration) budget comparable to the running time of our algorithm. Specifically, in our experiments, the normalized mean absolute error (NMAE) is typically between 0.02 and 0.3. The error measured this way generally decreases when increasing the size of the model which follows from the quadratic complexity of our algorithm. It is also decreasing in the magnitude of perturbations used: sampling is generally better at estimating larger quantities, whereas tiny perturbations lead to tiny prediction gaps.

1.1.2 PG^2 -based greedy feature ordering.

We also investigate the possibility of using our exact PG^2 algorithm as a base of a feature importance ranking algorithm. We stress that finding a feature ordering optimizing the PGI^2 metric is a highly non-trivial task, as the metric depends on the entire ordering of the features. Checking all the features’ permutations is infeasible in most cases.

We consider constructing the feature ranking using a *greedy* PG^2 heuristic: the i -th most important feature f is chosen so that it optimizes the prediction gap together with the already chosen $i - 1$ most important features plus f .

We next compare the greedy PG^2 ranking with the ranking produced using the popular SHAP feature attribution method for tree ensembles [LEC⁺20]. First of all, our experiments confirm that the greedy PG^2 ranking yields, on average, better PGI^2 scores than SHAP.

While that such a property holds is non-obvious, it is perhaps not very surprising either. This is why we also compare our ranking method with SHAP in terms of average *conciseness*. Specifically, we consider three natural metrics of averaged feature importance across the test data set, each of them based solely on the feature ordering and clearly promoting the most important features. For each of these metrics, we compare the entropy of the obtained averaged importances. Intuitively, a smaller entropy indicates that only few features are identified as critically important to the model.

Our experiments show that the greedy PG^2 ranking used with perturbations of sufficiently large standard deviation can lead to global importance scores with smaller entropy compared to SHAP.

2 Preliminaries

Let us denote by $f : \mathbb{R}^d \rightarrow \mathbb{R}$ the output function of the considered regression model. We sometimes also use f to refer to the model itself. The input $x \in \mathbb{R}^d$ to f is called a feature vector, and we denote by x_i the

value of the i -th feature of x . Thus, we identify the set of features with $[d]$.

Tree models. When talking about decision trees, we assume them to be binary and based on single-value splits. That is, each non-leaf node v of a decision tree \mathcal{T} has precisely two children a_v, b_v . It is also assigned a feature $q_v \in [d]$ and a threshold value $t_v \in \mathbb{R}$. Each leaf node $l \in \mathcal{T}$ is in turn assigned a value $y_l \in \mathbb{R}$. We denote by $\mathcal{L}(\mathcal{T})$ the set of leaves of the tree \mathcal{T} .

The output $f_{\mathcal{T}}(x)$ of the tree \mathcal{T} is computed by following a root-leaf path in \mathcal{T} : at a non-leaf node $v \in \mathcal{T}$, we descend either to the child a_v if $x_{q_v} < t_v$, or to b_v otherwise. When a leaf l is eventually reached, its value y_l is returned. We denote by $n_{\mathcal{T}}$ the number of nodes in \mathcal{T} .

When considering tree ensemble models $(\mathcal{T})_{i=1}^m$, the output $f(x)$ of the model is simply the sum of outputs $f_{\mathcal{T}_i}(x)$ of its m individual trees. We generally use $n = \sum_{i=1}^m n_{\mathcal{T}_i}$ to refer to the *total size* of the tree ensemble model.

Prediction gap on important feature perturbation. Let a *ranking* $\pi \in [d] \rightarrow [d]$ be a permutation of features giving their importance from highest to lowest. Denote by $\pi[1..\ell]$ the set $\{\pi(1), \dots, \pi(\ell)\}$, that is, the ℓ top ranking features in π . For any $x \in \mathbb{R}^d$ and $S \subseteq [d]$, let $\text{perturb}(x, S)$ be some distribution on feature vectors $x' \in \mathbb{R}^d$ satisfying $x'_i = x_i$ for all $i \notin S$. (**author?**) [AKS⁺22] define:

$$\text{PGI}(x, \pi, k) := \mathbb{E}_{x' \sim \text{perturb}(x, \pi[1..k])} [|f(x') - f(x)|].$$

Based on that, they define an averaged metric:

$$\text{PGI}(x, \pi) := \frac{1}{d} \sum_{k=1}^d \text{PGI}(x, \pi, k).$$

We analogously define the PGI^2 metric:

$$\begin{aligned} \text{PGI}^2(x, \pi, k) &:= \mathbb{E}_{x' \sim \text{perturb}(x, \pi[1..k])} \left[(f(x') - f(x))^2 \right], \\ \text{PGI}^2(x, \pi) &:= \frac{1}{d} \sum_{k=1}^d \text{PGI}^2(x, \pi, k). \end{aligned}$$

3 Computing PGI^2 for tree ensemble models

Consider distributions $\text{perturb}(x, S)$ such that $x' \sim \text{perturb}(x, S)$ satisfies:

1. for every $i \in S$, $x'_i = x_i + \delta_i$, where $\delta_i \sim \mathcal{D}_i$, and
2. all δ_j ($j \in S$) are independent random variables.

Moreover, we assume that for all $i \in S$, the c.d.f. $F_{\mathcal{D}_i}$ of \mathcal{D}_i can be evaluated in $O(1)$ time.

In the following, we show how to compute

$$\text{PG}^2(x, S) := \mathbb{E}_{x' \sim \text{perturb}(x, S)} [(f(x') - f(x))^2] \tag{1}$$

under the assumptions made in the case when f is a tree ensemble model $(\mathcal{T})_{i=1}^m$. Note that the metric $\text{PGI}^2(x, \pi)$ for a given ranking π can be computed by running the algorithm d times for different subsets S of the form $\pi[1..k]$.

Put $c = f(x)$. Let $x' \sim \text{perturb}(x, S)$. Recall that $f(x') = \sum_{i=1}^m f_{\mathcal{T}_i}(x')$. For every leaf node v of some \mathcal{T}_i , consider a random indicator variable X_v such that $X_v = 1$ iff \mathcal{T}_i evaluates to the value y_v of leaf v given x' as input. In particular, for any $i = 1, \dots, m$, there is exactly one $v \in \mathcal{L}(\mathcal{T}_i)$ such that $X_v = 1$. Set $\mathcal{L} = \bigcup_{i=1}^m \mathcal{L}(\mathcal{T}_i)$. Then:

$$f(x') = \sum_{v \in \mathcal{L}} X_v \cdot y_v.$$

By linearity of expectation, we obtain:

$$\begin{aligned}
\text{PG}^2(x, S) &= \mathbb{E} \left[\left(\sum_{v \in \mathcal{L}} X_v y_v - c \right)^2 \right] \\
&= c^2 + \mathbb{E} \left[\left(\sum_{u \in \mathcal{L}} X_u y_u \right) \left(\sum_{v \in \mathcal{L}} X_v y_v - 2c \right) \right] \\
&= c^2 + \sum_{\substack{u, v \in \mathcal{L} \\ u \neq v}} y_u y_v \Pr[X_u = 1 \wedge X_v = 1] \\
&\quad + \sum_{u \in \mathcal{L}} \Pr[X_u = 1] \cdot y_u \cdot (y_u - 2c).
\end{aligned}$$

The above formula reduces computing $\text{PG}^2(x, S)$ to calculating probabilities of the form $\Pr[X_u = 1 \wedge X_v = 1]$ (where $u \neq v$) or of the form $\Pr[X_u = 1]$. We focus on the former task as dealing with the latter is analogous but easier.

For a node w , let Q_w be the set of features appearing on the root- w path (in the tree whose w is the node of). Observe that for $w \in \mathcal{L}$, $X_w = 1$ holds iff for each feature $q \in Q_w$, x'_q falls into a certain interval $I_{w,q}$. Namely, if the root-to- w path consists of nodes $w_1, \dots, w_k = w$, then $I_{w,q}$ can be constructed as follows. Start with the interval $(-\infty, \infty)$, and follow the path downwards. For each encountered node w_i splitting on q , intersect the current $I_{w,q}$ with either:

- $(-\infty, t_{w_i})$ if $w_{i+1} = a_{w_i}$, or
- $[t_{w_i}, \infty)$ if $w_{i+1} = b_{w_i}$, or
- \emptyset otherwise.

It follows that $X_u = 1 \wedge X_v = 1$ iff for all $q \in Q_u \cup Q_v$, $x'_q \in I_{u,q} \cap I_{v,q}$. Hence, if we denote by $l_{u,v,q}, r_{u,v,q}$ the respective endpoints of $I_{u,q} \cap I_{v,q}$, by the independence of all perturbations δ_j , we obtain that $\Pr[X_u = 1 \wedge X_v = 1]$ equals $\Pi(u, v)$, where

$$\Pi(u, v) = \left(\prod_{q \in (Q_u \cup Q_v) \setminus S} [x_q \in I_{u,q} \cap I_{v,q}] \right) \cdot \left(\prod_{q \in (Q_u \cup Q_v) \cap S} (F_{\mathcal{D}_q}(r_{u,v,q} - x_q) - F_{\mathcal{D}_q}(l_{u,v,q} - x_q)) \right). \quad (2)$$

Implemented naively, computing a single value $\Pi(u, v)$ takes $O(D_u + D_v)$ time, where D_u, D_v are the depths of u and v in their respective trees. Indeed, note that by traversing the root-to- u and root-to- v paths, we can find all the relevant intervals $I_{u,q}, I_{v,q}$ that the product $\Pi(u, v)$ depends on. Moreover, $\Pi(u, v)$ has at most $D_u + D_v$ factors, each of which can be evaluated in $O(1)$ time.

Computing the values $\Pi(u, v)$ through all $\Theta(n^2)$ pairs $u, v \in \mathcal{L}$ could take $O(n^2 D)$ time, where D is a global bound on the depth of the trees in the ensemble.

However, the computation can be optimized to run in $O(n^2)$ time by computing the probabilities in an adequate order. Namely, note that, say, the value $\Pi(a_u, v)$ can be computed based on $\Pi(u, v)$ in $O(1)$ time. This is because the interval $I_{a_u,q}$ can differ from the corresponding interval $I_{u,q}$ only for the feature $q = q_u$, and it can be obtained by splitting $I_{u,q}$ with the threshold t_u . Hence, only one factor of the product (2) has to be added or replaced in order to obtain $\Pi(a_u, v)$ from $\Pi(u, v)$. An analogous trick applies to computing $\Pi(b_u, v)$, $\Pi(u, a_v)$, $\Pi(u, b_v)$ from $\Pi(u, v)$. Consequently, by iterating through nodes u in pre-order, and then, once $u \in \mathcal{L}$ is fixed, through nodes v in pre-order (the order of processing trees does not matter), all the required values $\Pi(u, v)$ can be computed in $O(n^2)$ total time.

Theorem 3.1. *Let f be a tree ensemble model whose trees have n nodes in total. Let $x \in \mathbb{R}^d$. Then for any $S \subseteq [d]$, $\text{PG}^2(x, S)$ can be computed in $O(n^2)$ time. In particular, given a feature ranking π , for any $k \in [d]$, $\text{PGI}^2(x, \pi, k)$ can be computed in $O(n^2)$ time, whereas $\text{PGI}^2(x, \pi)$ can be computed in $O(n^2 d)$ time.*

4 Experiments

4.1 Datasets

Following the previous work (e.g., [AKS⁺22, DUA⁺22]), in the experiments we assume that the (real) perturbations used for computing the prediction gap (either exactly, or approximately) come from the same normal distribution $\mathcal{D} = \mathcal{N}(0, \sigma^2)$. This is why we need to assume that all the features have numerical values.

Using the same perturbation distribution for all the features requires the features be standardised by subtracting the mean and dividing by the standard deviation. This ensures that if a feature is perturbed by a noise variable drawn from \mathcal{D} , the perturbation will have a similar effect. More specifically, it prevents a perturbation from \mathcal{D} being relatively significant for one feature and insignificant for another.

In our experiments we used two datasets:

1. Red Wine Quality Dataset [CCA⁺09] The dataset contains 11 features related to physico-chemical attributes of wine, all numerical and continuous. The task is to predict the score of a wine, which is an integer between 1 and 10. The task can be considered as both a regression and a classification task. The dataset contains 1 599 examples.
2. California Housing [Tor23] The dataset contains information from the 1990 Californian census on some characteristics of a given Californian county and the median house value in that county. There are 8 numerical characteristics, such as length or number of bedrooms, and one categorical characteristic - proximity to the ocean. For the reasons outlined before, we decided to drop this feature and use a modified dataset. The task is to predict the median value of the house. The dataset contains 20 640 examples.

4.2 Models

All tree ensembles are implemented in the XGBoost library [CG16]. For each of the two datasets, three models of the following types were trained:

- Single tree – a single decision tree with `max_depth` set to 4.
- Bigger – gradient boosted trees with `max_depth` set to 4 and number of trees limited to 40.

In each case, the data set was split 80:20 into training and test sets. In addition, for each model and its constraint, a grid search was performed over selected hyperparameters. The details of the training process can be found in Appendix B.

4.3 Comparing squared prediction gap algorithms

In this section we compare our algorithm computing the squared prediction gap (as defined in Equation (1)) for tree ensembles described in Section 3 and the Monte Carlo sampling-based method. Specifically, the latter algorithm, given x and the set $S \subseteq [d]$ or perturbed features, evaluates $f(x')$ for i randomly sampled $x' \sim \text{perturb}(x, S)$ (see Section 3) and records the average value of $(f(x') - f(x))^2$. We will call i the number of *iterations* in the following.

The subject of the comparison was the accuracy of the results produced by the sampling algorithm. Since the accuracy of the sampling algorithm increases with the number of iterations i , to make the comparison fair, the number i was chosen so that the wall time of both algorithms was close. Both algorithms were implemented in Python and all the arithmetic operations in the algorithms were carried out using the `numpy.float32` type.

The computations were carried out on a FormatServer THOR E221 (Supermicro) server equipped with two AMD EPYC 7702 64-Core processors and 512 GB of RAM with operation system Ubuntu 22.04.1 LTS.

The comparison between the algorithms was carried out in different settings. The variable parameters were:

- Model type m trained on a selected dataset. In our case, there were four models in total (Section 4.2) trained on two datasets (Section 4.1).
- The standard deviation σ of a Gaussian used to perturb a feature. In our experiment, the evaluated values were $\{0.01, 0.03, 0.1, 0.3\}$.

To carry out the experiment having fixed the above parameters, we used the following procedure. For each number of iterations $i \in \{100, 500, 1000, 1500, 2000, 3000, 4000, 5000, 6000\}$, we recorded the average differences in results and computation times over $N = 20\,000$ samples. These samples varied in the size of the perturbed feature set S (which could be, e.g., $1, \dots, 11$ for the Wine Quality dataset), and we ensured that all subset sizes were equally represented in the samples. Each sample involved a randomly selected point from a test dataset and a set of features of the desired size. Both algorithms were then run with appropriate parameters on each prepared sample. We compared the running times and results of the two algorithms. The error was recorded as the Normalised Mean Absolute Error (NMAE), defined as:

$$\text{NMAE}(y, \hat{y}) = \frac{\sum_{j=1}^N |y_j - \hat{y}_j|}{\sum_{j=1}^N |y_j|}$$

where y_j is the correct value of the prediction gap calculated by the exact algorithm, \hat{y}_j is the prediction gap calculated by the sampling algorithm. NMAE was used as opposed to the relative error to suppress the effect of relatively large floating-point errors present when operating on very small numbers.

The results obtained in the experiment – the error as a function of the number of iterations – are depicted using the “Mean” curve for $\sigma = 0.3$ and Bigger model for the Red Wine Quality dataset in Figure 1 and for $\sigma = 0.03$ and Bigger model for the Californian Housing dataset in Figure 2. Analogous figures for other settings (m, σ) can be found in Appendix B.

Additionally, the figures contain separate error curves for some selected sizes $|S|$ of the perturbed features set. As can be observed for a given iteration, the NMAE error behaves similarly for all subset sizes. Overall, the difference between the exact and sampling algorithms decreases as the number of iterations in the sampling algorithm increases. This is indeed anticipated since Monte Carlo sampling yields better accuracy with iteration increase; in fact the relative error decreases proportionally to $1/\sqrt{i}$.

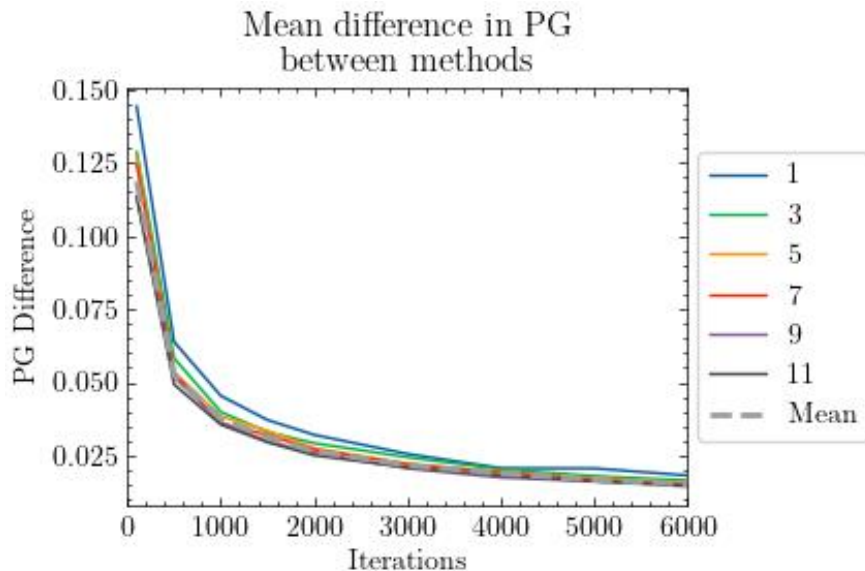


Figure 1: Results of precision comparison described in 4.3 for $\sigma = 0.3$ and for Bigger model for Red Wine Quality dataset.

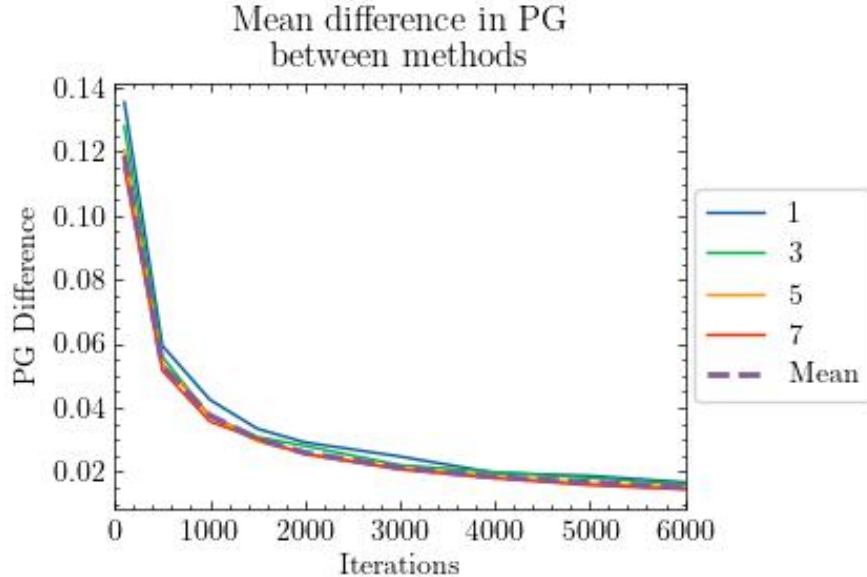


Figure 2: Results of precision comparison described in 4.3 for $\sigma = 0.03$ and for Bigger model for California housing dataset.

Table 1: Number of iterations needed to perform to match execution time of exact algorithm on single tree model for Wine Quality Dataset described in 4.3.

σ	Number of iterations	Relative error
0.01	100	0.08
0.03	100	0.14
0.1	100	0.15
0.3	1000	0.05

For the fair comparison, we chose the number of iterations (out of 9 considered as explained above) in the sampling algorithm that came closest to the running time of the exact algorithm for each setting. The chosen number of iterations and the associated NMAE are shown in Tables 1, 2, 3 4.

We conclude that the “fair” comparison confirms that the Monte Carlo simulation gives noticeably less accurate results than our exact method. We observe that the error generally decreases when increasing the size of the model. This is justified by the fact that our algorithm’s running time increases quadratically with n , whereas a single iteration of the Monte Carlo method runs in time at most linear in n . As a result, the bigger the model size is, the more iterations the Monte Carlo method can perform within the same time budget. Moreover, the error decreases with the standard deviation of the distribution used to obtain perturbations. This is also expected: for smaller perturbations, the floating-point rounding errors are of higher significance.

5 Feature ranking using PG^2

We propose a method for ranking the features of a model using the squared prediction gap called *greedy* PG^2 . Let $x \in \mathbb{R}^d$. Suppose the feature perturbations δ_i all come from $\mathcal{D} = \mathcal{N}(0, \sigma)$. The ranking $\pi_{\text{PG}}^\sigma(x)$ is constructed in the following inductive manner.

1. For every $i \in [d]$, compute $p_i = \text{PG}^2(x, \{i\})$. Set the most important feature $\pi_{\text{PG}}^\sigma(x)(1)$ to be the

Table 2: Number of iterations needed to perform to match execution time of exact algorithm on Bigger model for Wine Quality Dataset described in 4.3.

σ	Number of iterations	Relative error
0.01	100	0.08
0.03	100	0.11
0.1	100	0.12
0.3	1000	0.04

Table 3: Number of iterations needed to perform to match execution time of exact algorithm on single tree model for Californian Housing dataset described in 4.3.

σ	Number of iterations	Relative error
0.01	100	0.13
0.03	100	0.15
0.1	100	0.15
0.3	1000	0.04

Table 4: Number of iterations needed to perform to match execution time of exact algorithm on Bigger tree model for Californian Housing dataset described in 4.3.

σ	Number of iterations	Relative error
0.01	500	0.3
0.03	500	0.14
0.1	1000	0.06
0.3	2000	0.03

Table 5: Number of iterations needed to perform to match execution time of exact algorithm on Bigger Californian Housing model described in 4.3.

σ	Number of iterations	Relative error
0.01	500	0.30
0.03	500	0.14
0.1	1000	0.06
0.3	2000	0.03

feature i for which p_i is the highest.

2. Assume $\pi_{\text{PG}}^\sigma(x)(1), \dots, \pi_{\text{PG}}^\sigma(x)(l)$ are already computed. Let $S = \{\pi_{\text{PG}}^\sigma(x)(1), \dots, \pi_{\text{PG}}^\sigma(x)(l)\}$. For every $i \in [d] \setminus S$, compute $p_i := \text{PG}^2(x, S \cup \{i\})$. Let the next important feature $\pi_{\text{PG}}^\sigma(x)(l+1)$ be the feature i for which p_i is the highest.

In the following, we compare the feature rankings obtained using the above method with the rankings obtained using the popular SHAP attribution framework [LEC⁺20].

For a given $x \in \mathbb{R}^d$, SHAP produces an attribution vector $(\phi)_{i=1}^d$ whose elements sum up to $f(x) - \mathbb{E}[f(x)]$ but can be both positive and negative [LL17]. We define the ranking $\pi_{\text{SHAP}}(x)$ to be obtained by sorting the features $[d]$ by the *absolute value* of ϕ_i , from highest to lowest. This is justified by the fact that the predictions $f(x)$ can be smaller than the expected value; in such a case, all the attributions ϕ_i might be negative.

5.1 Global comparison vs SHAP wrt. PGI^2

We perform a *global* comparison of π_{PG}^σ and π_{SHAP} wrt. the PGI^2 metric, that is, we check which ranking method gives higher PGI^2 scores on average. More formally, fix a dataset/model combination m and a perturbation distribution $\mathcal{D}' = \mathcal{N}(0, \sigma')$, where potentially $\sigma' \neq \sigma$, as we did in Section 4.3. Let $X \subseteq \mathbb{R}^d$ be the corresponding dataset used in m . Then, define the average PGI^2 scores as

$$\begin{aligned} \overline{\text{PGI}^2}(\pi_{\text{SHAP}}) &= \frac{1}{|X|} \sum_{x \in X} \text{PGI}^2(x, \pi_{\text{SHAP}}(x)), \\ \overline{\text{PGI}^2}(\pi_{\text{PGI}}^\sigma) &= \frac{1}{|X|} \sum_{x \in X} \text{PGI}^2(x, \pi_{\text{PGI}}^\sigma(x)). \end{aligned}$$

Figures 3, 4, 5 and 6 present the comparison of the average scores $\overline{\text{PGI}^2}(\pi_{\text{SHAP}})$ and $\overline{\text{PGI}^2}(\pi_{\text{PGI}}^\sigma)$ for $\sigma = 0.3$ as a function of σ' . We observe that even if the parameter σ used when computing the ranking π_{PG}^σ differs from the parameter σ' used for computing the PGI^2 metrics, $\overline{\text{PGI}^2}(\pi_{\text{PGI}}^\sigma)$ is consistently better than $\overline{\text{PGI}^2}(\pi_{\text{SHAP}})$ for the Bigger models. For Single tree models, this is the case only for sufficiently large σ' , but in particular for $\sigma' = \sigma$. The figures presenting the results for other choices of σ can be found in Appendix B.2.

We conclude that the greedy optimization of the $\text{PGI}^2(x, \pi)$ metric performs reasonably well, even though its correctness could only be guaranteed if it optimized the $\text{PGI}^2(x, \pi, 1)$ metric (see Section 2) instead.

5.2 Conciseness comparison vs SHAP

We also compare the global conciseness of the feature rankings π_{SHAP} and π_{PG}^σ . Intuitively, we would like to declare a feature ranking method more concise if it tends to produce rankings that identify the most important features of the model more clearly. For example, the information that two or three features of the model are identified as much more important than the others seems to say more about the model's behavior in general than saying that all the features are equally important on average.

Our conciseness evaluation is performed using four different methods of converting a feature ranking $\pi(x)$ to a score vector $r^\pi(x) : [d] \rightarrow \mathbb{R}_{\geq 0}$: *geom*, *top1*, *top2*, *top3*:

- *geom* sets $(r^\pi(x))_i = 1/2^k$ if $\pi(k) = i$, that is, the scores increase geometrically with the importance.
- *topk*, for $k \in \{1, 2, 3\}$, sets $(r^\pi(x))_i = 1$ iff $i \in \{\pi(1), \dots, \pi(k)\}$. In other words, the top k features get a unit score, and all others get a zero score.

Having fixed (as before) the model-dataset combination m , σ , and a scoring method, we compute the aggregate feature scores R_i through all data points x from the test dataset X :

$$R_i = \sum_{x \in X} (r^\pi(x))_i.$$

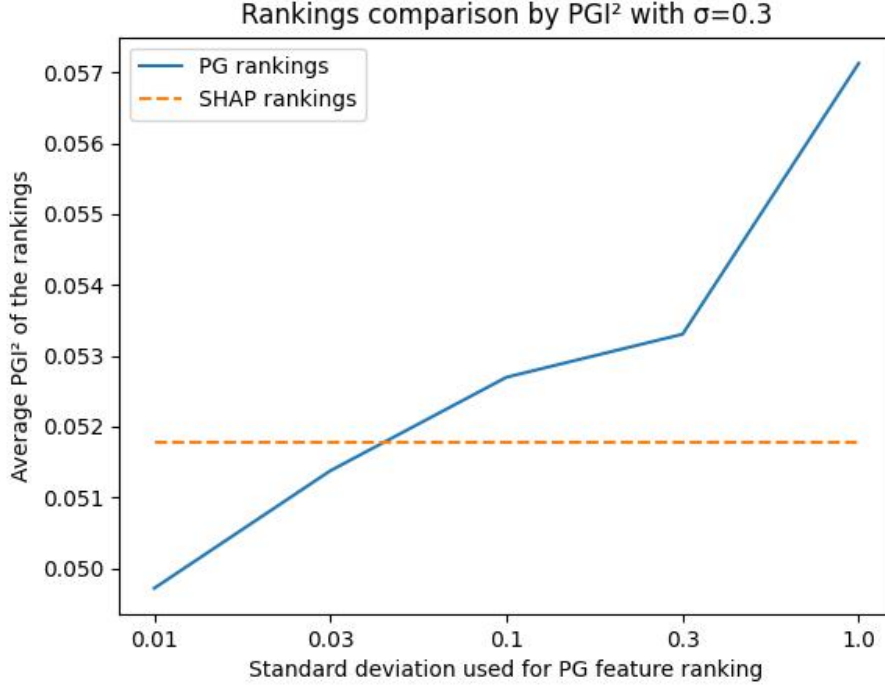


Figure 3: Single tree model for the Wine Quality dataset.

Finally, the conciseness C_π is computed as the entropy of the normalized vector R_1, \dots, R_d :

$$C_\pi = \sum_{i=1}^d \frac{R_i}{\sum_j R_j} \log \left(\frac{R_i}{\sum_j R_j} \right).$$

Intuitively, higher entropy means more uncertainty in the results.

Tables 6,7, 8, and 9 present the results of our comparison for $\sigma \in \{0.1, 0.3\}$ for Wine Quality models, and additionally for $\sigma = 1$ for the Housing models. We observe that for the “single tree” models, the entropy that SHAP ranking yields is slightly smaller, for most of the scoring methods. However, there is not much uncertainty in the produced rankings since the models base their predictions only on a few features. Indeed, in the case of “single tree” models for both Wine Quality and Californian Housing datasets, only three features were present in trees.

For the bigger models consisting of numerous trees, all the features are used. In this more complex case, where the top features are not identified immediately, the greedy PG-based ranking yields more concise rankings for the *geom*, *top2* and *top3* metrics for the Wine Quality dataset. For the Housing dataset, however, the obtained entropies for π_{SHAP} are also consistently smaller than for the π_{PG}^σ rankings for $\sigma \in \{0.1, 0.3\}$. Only for $\sigma = 1$, the greedy PG^2 method looks generally more concise.

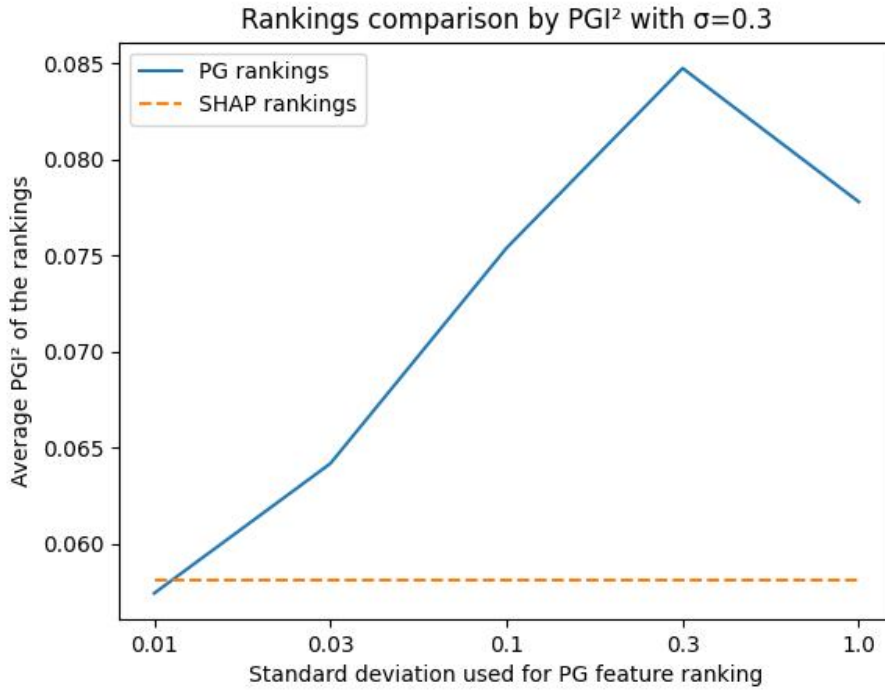


Figure 4: Bigger model for the Wine Quality dataset.

Table 6: Entropy comparison between SHAP rankings and PG rankings for Bigger model for Wine Quality Dataset.

score	SHAP	PG $\sigma = 0.1$	PG $\sigma = 0.3$	PG $\sigma = 1.0$
<i>geom</i>	3.245	3.285	3.157	2.740
<i>top1</i>	2.643	3.059	2.792	1.730
<i>top2</i>	3.120	3.232	3.019	2.402
<i>top3</i>	3.305	3.300	3.189	2.846

Table 7: Entropy comparison between SHAP rankings and PG rankings for Bigger model for Californian Housing Dataset.

score	SHAP	PG $\sigma = 0.1$	PG $\sigma = 0.3$	PG $\sigma = 1.0$
<i>geom</i>	2.570	2.774	2.624	2.383
<i>top1</i>	1.748	2.324	1.979	0.534
<i>top2</i>	2.394	2.651	2.377	2.176
<i>top3</i>	2.634	2.834	2.676	2.622

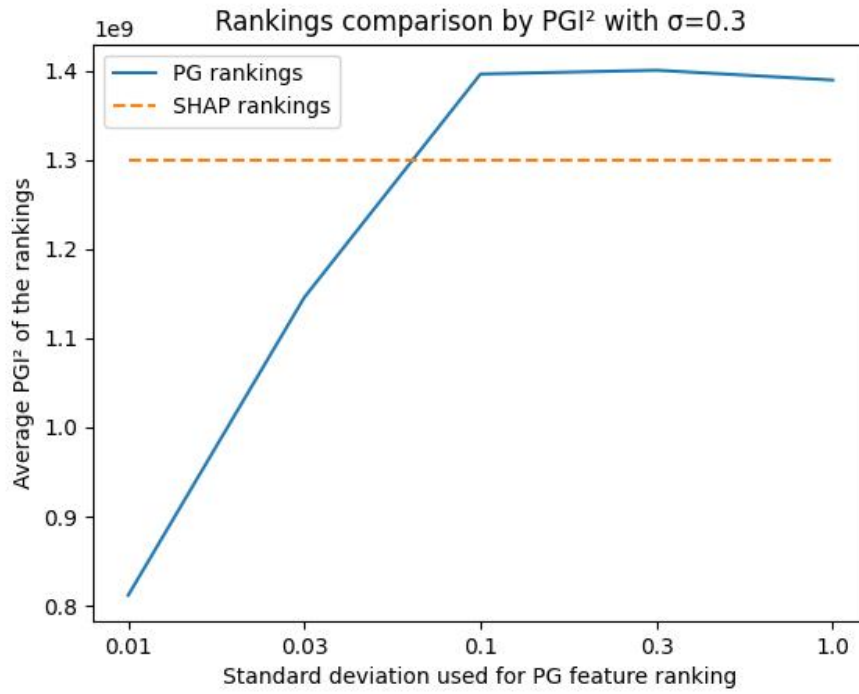


Figure 5: Single tree model for the Housing dataset.

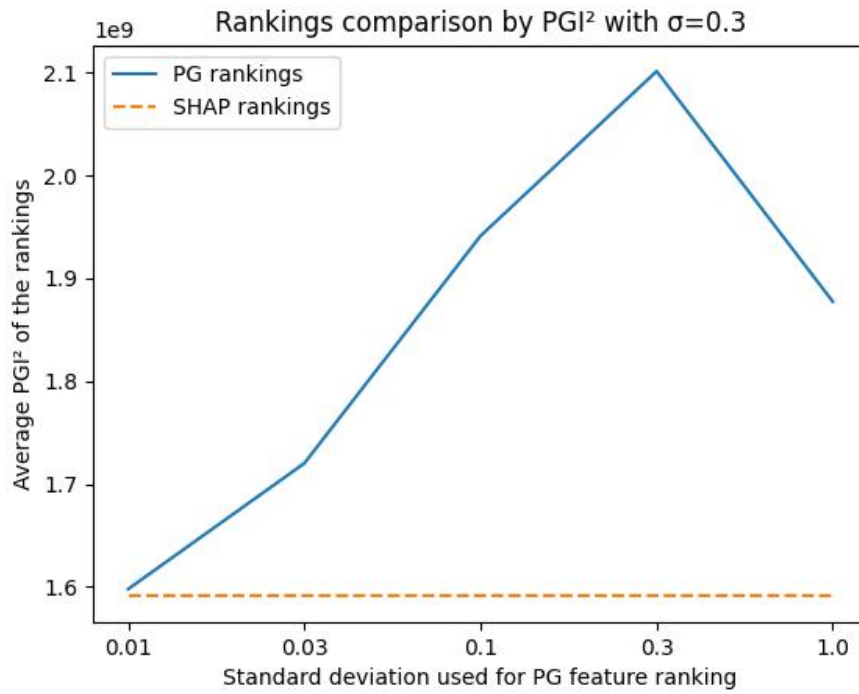


Figure 6: Bigger model for the Housing dataset

Table 8: Entropy comparison between SHAP rankings and PG rankings for Single tree model for Wine Quality Dataset.

score	SHAP	PG, $\sigma = 0.1$	PG, $\sigma = 0.3$	PG, $\sigma = 1.0$
<i>geom</i>	2.644	2.463	2.328	2.316
<i>top1</i>	1.725	1.482	1.372	1.305
<i>top2</i>	2.112	1.988	1.654	1.585
<i>top3</i>	2.432	2.207	2.073	2.012

Table 9: Entropy comparison between SHAP rankings and PG rankings for Single tree model for Californian Housing Dataset.

score	SHAP	PG $\sigma = 0.1$	PG $\sigma = 0.3$	PG $\sigma = 1.0$
<i>geom</i>	2.094	2.197	2.175	2.138
<i>top1</i>	1.077	0.884	0.722	0.031
<i>top2</i>	1.549	1.580	1.602	1.633
<i>top3</i>	1.585	1.998	2.020	2.066

References

- [AKS⁺22] Chirag Agarwal, Satyapriya Krishna, Eshika Saxena, Martin Pawelczyk, Nari Johnson, Isha Puri, Marinka Zitnik, and Himabindu Lakkaraju. Openxai: Towards a transparent evaluation of model explanations. *Advances in Neural Information Processing Systems*, 35:15784–15799, 2022.
- [AMJ18] David Alvarez-Melis and Tommi S Jaakkola. On the robustness of interpretability methods. *arXiv preprint arXiv:1806.08049*, 2018.
- [BH21] Nadia Burkart and Marco F. Huber. A survey on the explainability of supervised machine learning. *J. Artif. Intell. Res.*, 70:245–317, 2021.
- [BZH⁺22] Aparna Balagopalan, Haoran Zhang, Kimia Hamidieh, Thomas Hartvigsen, Frank Rudzicz, and Marzyeh Ghassemi. The road to explainability is paved with bias: Measuring the fairness of explanations. In *Proceedings of the 2022 ACM Conference on Fairness, Accountability, and Transparency*, pages 1194–1206, 2022.
- [CCA⁺09] Paulo Cortez, A. Cerdeira, F. Almeida, T. Matos, and J. Reis. Wine Quality. UCI Machine Learning Repository, 2009. DOI: <https://doi.org/10.24432/C56S3T>.
- [CG16] Tianqi Chen and Carlos Guestrin. Xgboost: A scalable tree boosting system. In *Proceedings of the 22nd ACM SIGKDD International Conference on Knowledge Discovery and Data Mining*, KDD '16. ACM, August 2016.
- [DJR⁺20] Jay DeYoung, Sarthak Jain, Nazneen Fatema Rajani, Eric Lehman, Caiming Xiong, Richard Socher, and Byron C. Wallace. ERASER: A benchmark to evaluate rationalized NLP models. In *Proceedings of the 58th Annual Meeting of the Association for Computational Linguistics, ACL 2020, Online, July 5-10, 2020*, pages 4443–4458. Association for Computational Linguistics, 2020.
- [DUA⁺22] Jessica Dai, Sohini Upadhyay, Ulrich Aivodji, Stephen H Bach, and Himabindu Lakkaraju. Fairness via explanation quality: Evaluating disparities in the quality of post hoc explanations. In *Proceedings of the 2022 AAAI/ACM Conference on AI, Ethics, and Society*, pages 203–214, 2022.
- [HEKK19] Sara Hooker, Dumitru Erhan, Pieter-Jan Kindermans, and Been Kim. A benchmark for interpretability methods in deep neural networks. In *Advances in Neural Information Processing Systems 32: Annual Conference on Neural Information Processing Systems 2019, NeurIPS 2019, December 8-14, 2019, Vancouver, BC, Canada*, pages 9734–9745, 2019.
- [LEC⁺20] Scott M. Lundberg, Gabriel G. Erion, Hugh Chen, Alex J. DeGrave, Jordan M. Prutkin, Bala Nair, Ronit Katz, Jonathan Himmelfarb, Nisha Bansal, and Su-In Lee. From local explanations to global understanding with explainable AI for trees. *Nat. Mach. Intell.*, 2(1):56–67, 2020.
- [LKWN21] Yang Liu, Sujay Khandagale, Colin White, and Willie Neiswanger. Synthetic benchmarks for scientific research in explainable machine learning. In *Proceedings of the Neural Information Processing Systems Track on Datasets and Benchmarks 1, NeurIPS Datasets and Benchmarks 2021, December 2021, virtual*, 2021.
- [LL17] Scott M Lundberg and Su-In Lee. A unified approach to interpreting model predictions. In *Advances in Neural Information Processing Systems*, volume 30. Curran Associates, Inc., 2017.
- [PDS18] Vitali Petsiuk, Abir Das, and Kate Saenko. RISE: randomized input sampling for explanation of black-box models. In *British Machine Vision Conference 2018, BMVC 2018, Newcastle, UK, September 3-6, 2018*, page 151. BMVA Press, 2018.

- [PMT18] Gregory Plumb, Denali Molitor, and Ameet Talwalkar. Model agnostic supervised local explanations. In *Advances in Neural Information Processing Systems 31: Annual Conference on Neural Information Processing Systems 2018, NeurIPS 2018, December 3-8, 2018, Montréal, Canada*, pages 2520–2529, 2018.
- [RSG16] Marco Túlio Ribeiro, Sameer Singh, and Carlos Guestrin. "Why should I trust you?": Explaining the predictions of any classifier. In *Proceedings of the 22nd ACM SIGKDD International Conference on Knowledge Discovery and Data Mining, San Francisco, CA, USA, August 13-17, 2016*, pages 1135–1144. ACM, 2016.
- [Tor23] Luis Torgo. California housing dataset. https://www.dcc.fc.up.pt/~ltorgo/Regression/cal_housing.html, 2023. Accessed on: October 10, 2023.
- [YHS⁺19] Chih-Kuan Yeh, Cheng-Yu Hsieh, Arun Suggala, David I Inouye, and Pradeep K Ravikumar. On the (in) fidelity and sensitivity of explanations. *Advances in Neural Information Processing Systems*, 32, 2019.

A Models training

The grid search was performed by using class *GridSearchCV* from library XGBoost [CG16] with numbers of folds in cross-validation set to 5. Additionally to parameters described in 4.2, the grid search included also parameters with the following possible values:

- *eta* with possible values in $\{0.01, 0.1, 0.2, 0.3, 0.4, 0.5, 0.6, 0.7, 0.8, 0.9\}$
- *subsample* with possible values in $0.01, 0.1, 0.2, 0.3, 0.4, 0.5, 0.6, 0.7, 0.8, 0.9$

B Additional experiments results

B.1 Results from precision experiments

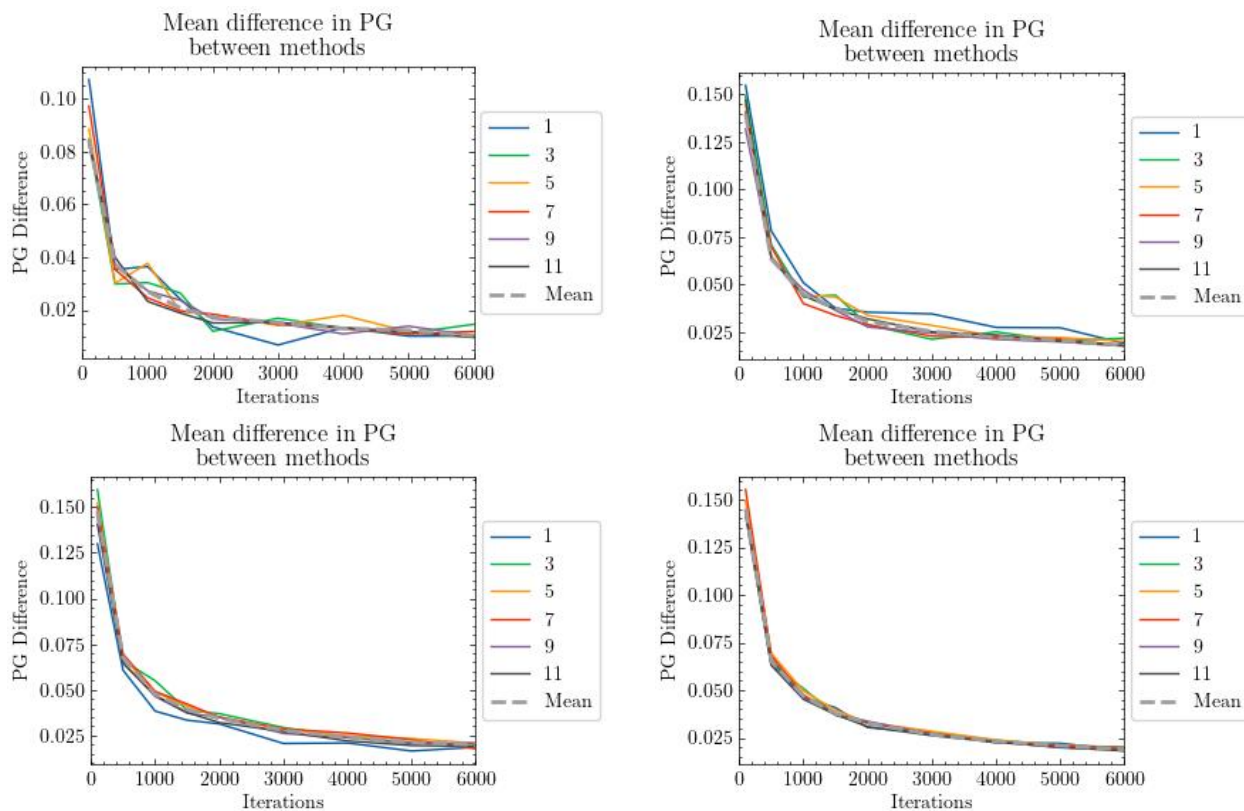


Figure 7: Single tree model for Wine Quality dataset

B.2 Results from PGI comparison experiment

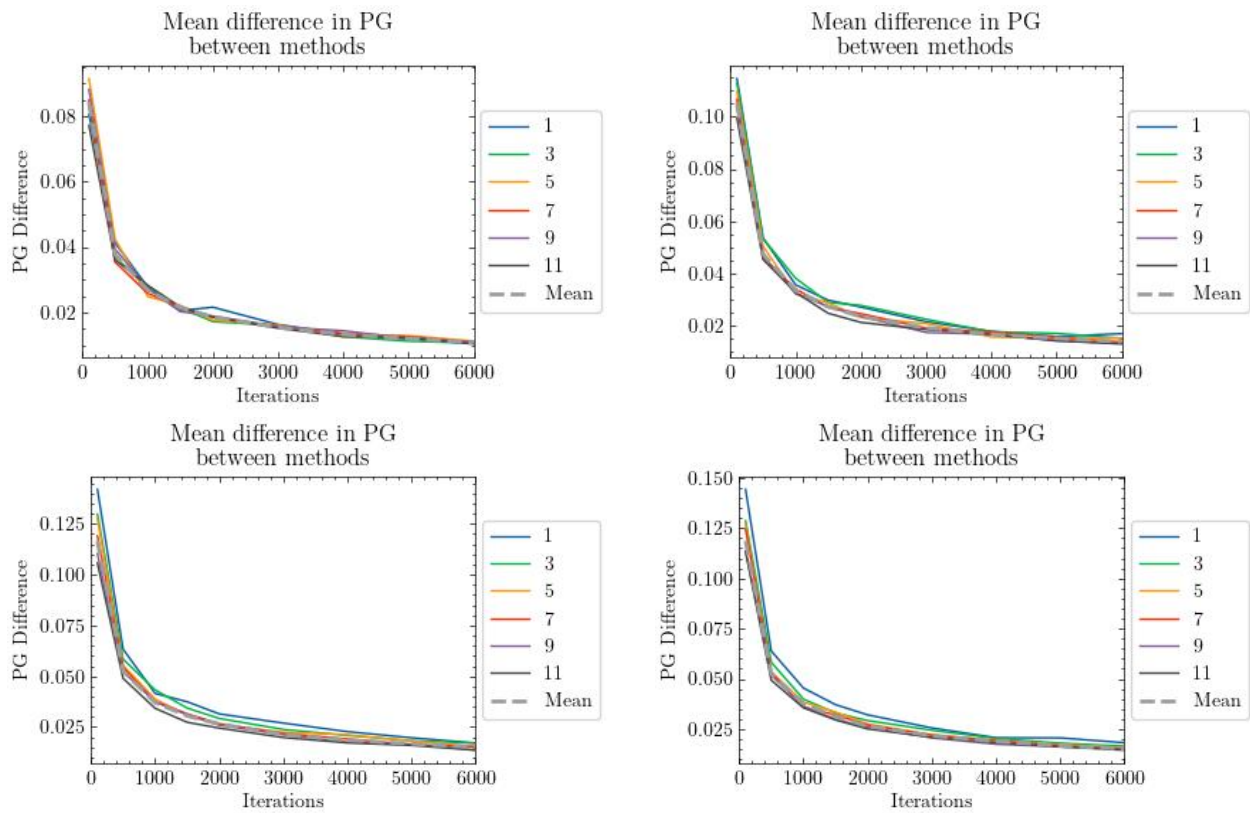


Figure 8: Bigger model for Wine Quality dataset

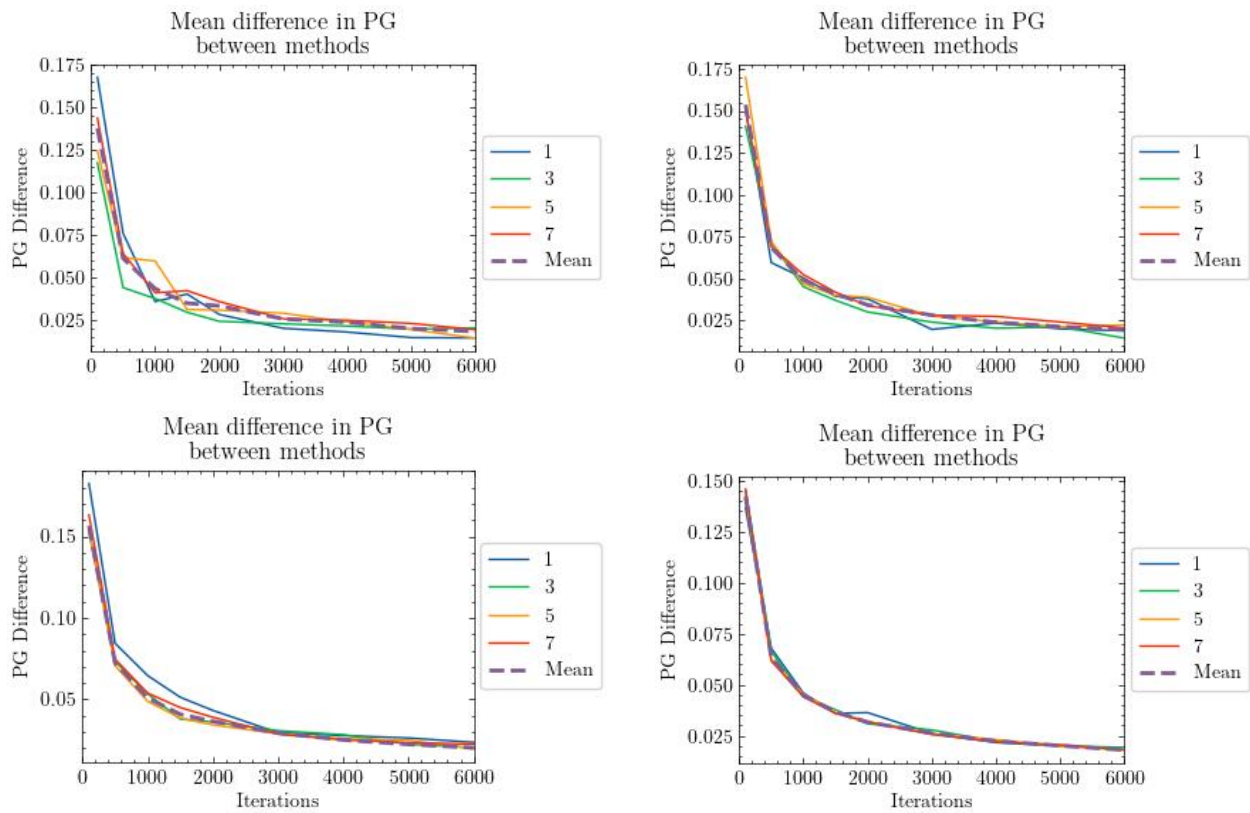


Figure 9: Single tree model for Californian Housing dataset

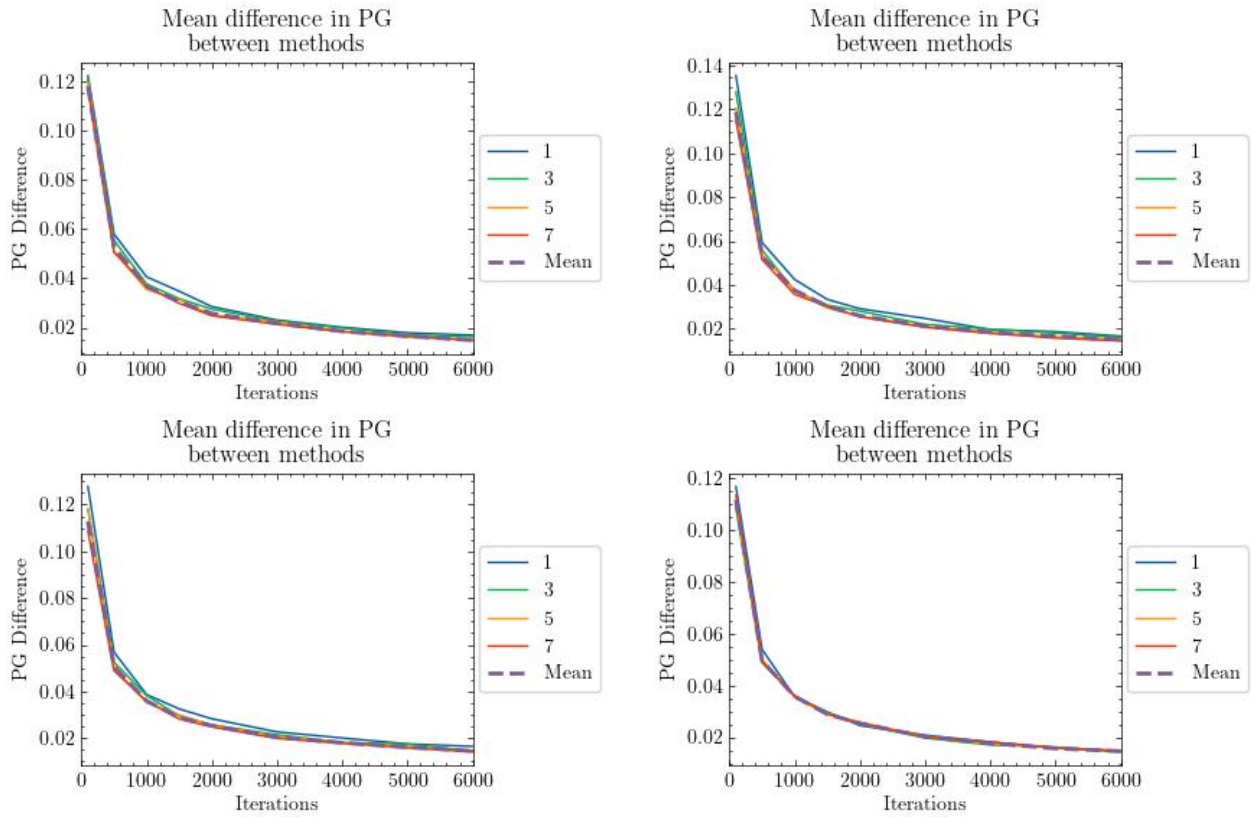


Figure 10: Bigger model for Californian Housing dataset

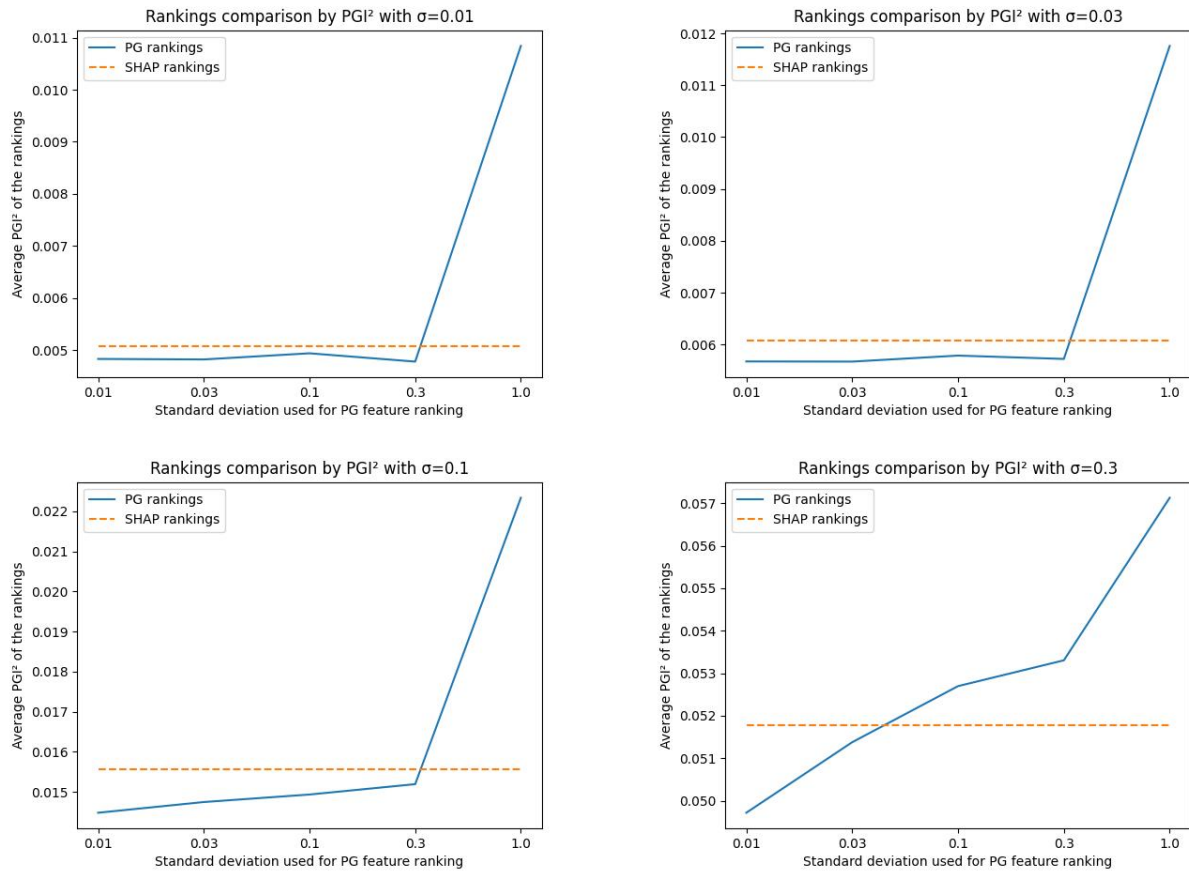


Figure 11: Single tree model for the Wine Quality dataset.

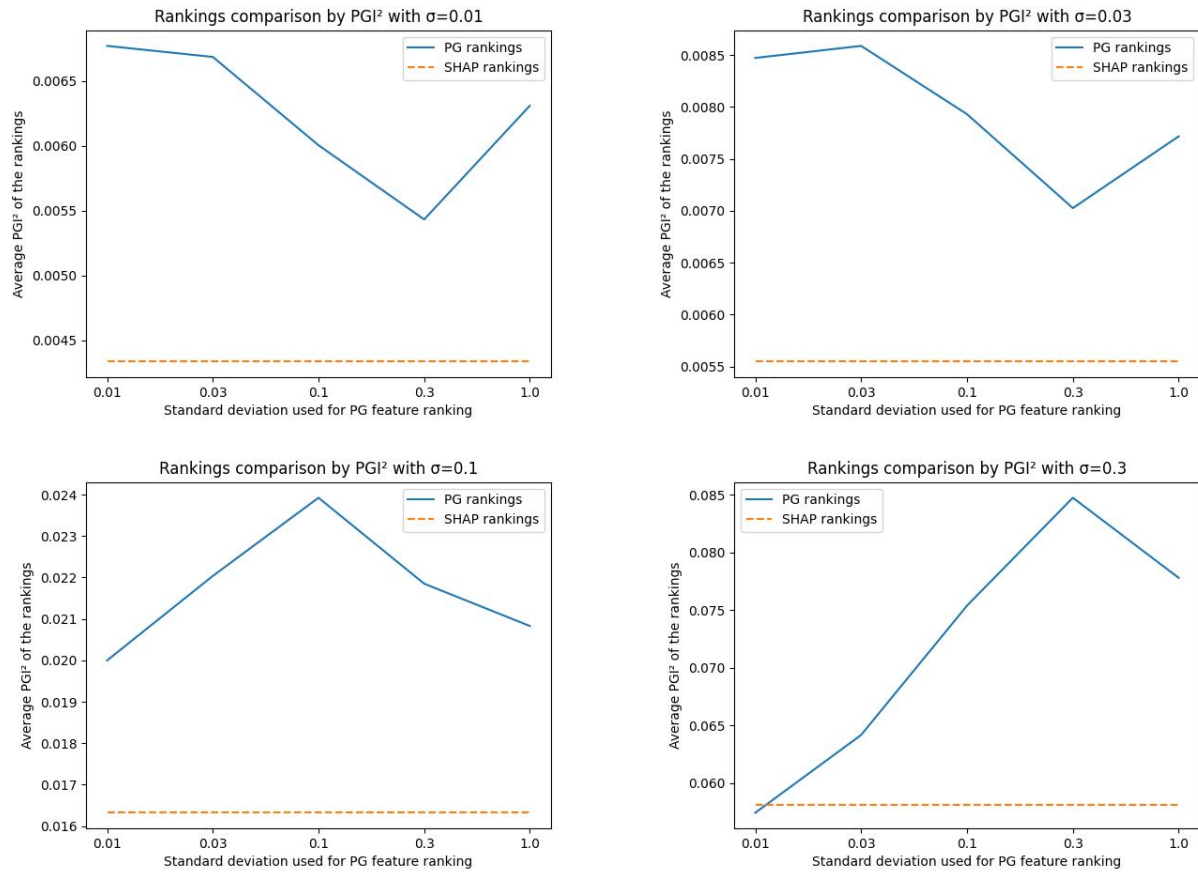


Figure 12: Bigger model for the Wine Quality dataset.

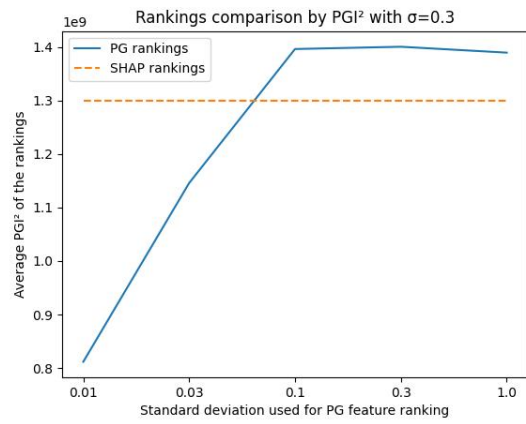
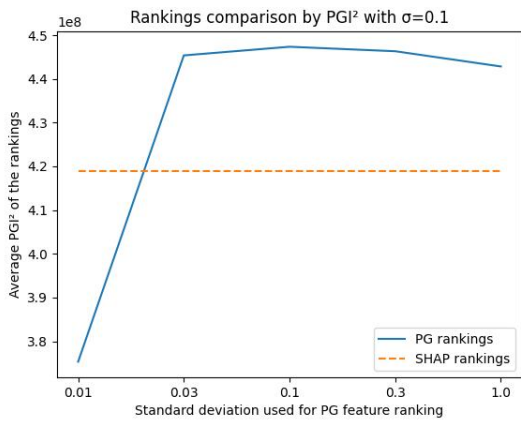
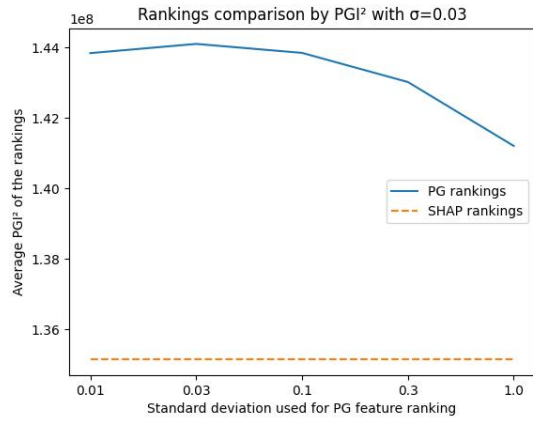
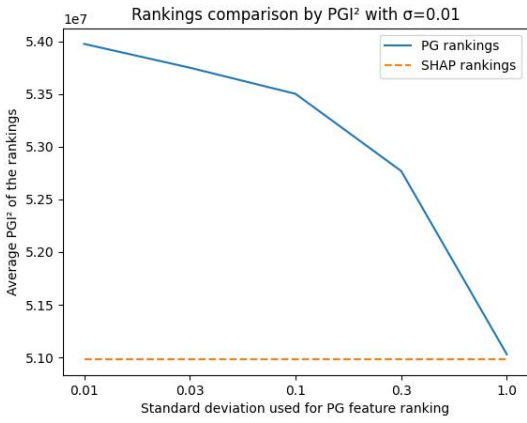


Figure 13: Single tree model for Californian Housing dataset

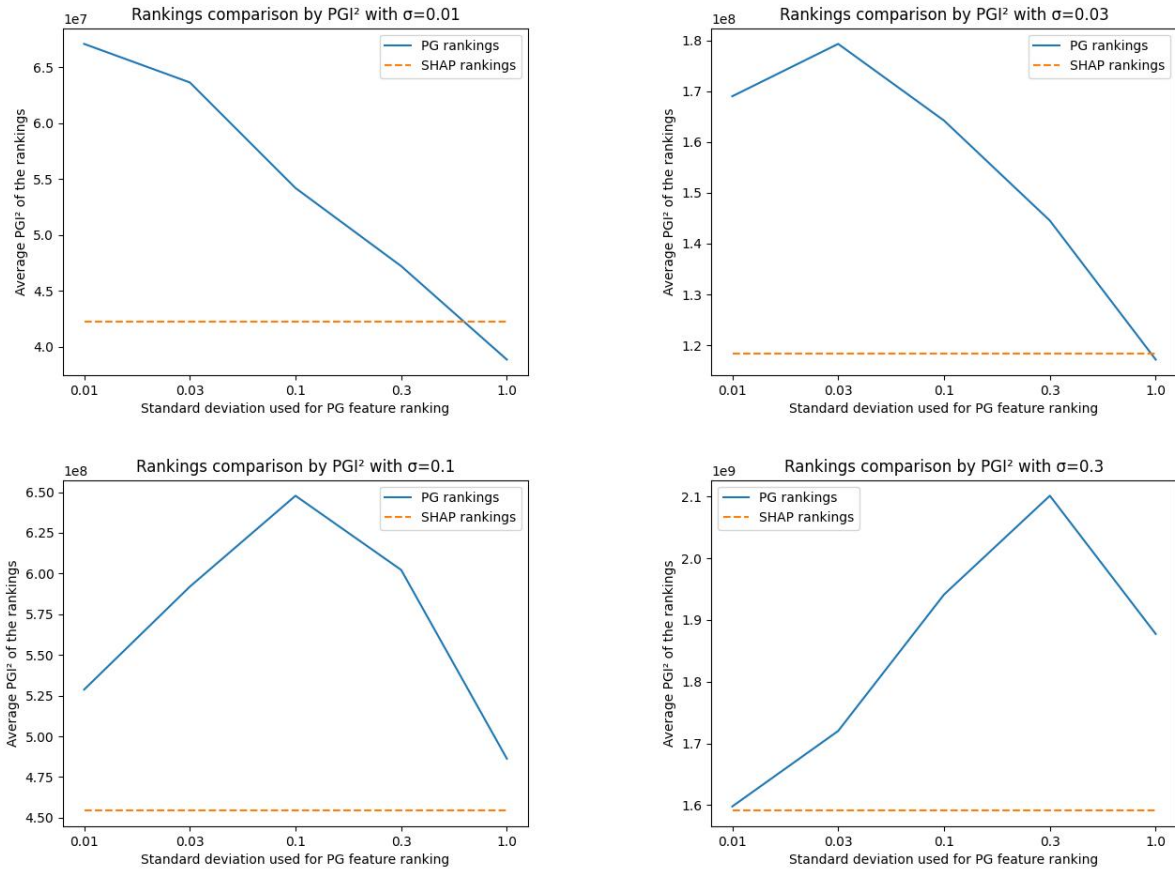


Figure 14: Bigger model for Californian Housing dataset